Received: 25 April 2024 | Revised: 27 May 2024 | Accepted: 3 June 2024

DOI: 10.1002/pol.20240336

RESEARCH ARTICLE

JOURNAL OF POLYMER SCIENCE WILEY

Supramolecular hydrogels based on hydrogen bonding: Impact of ionic comonomers

Amir Jangizehi | **Cora Sprenger** | **Sebastian Seiffert**

Department of Chemistry, Johannes Gutenberg University of Mainz, Mainz, Germany

Correspondence
Sebastian Seiffert, Department of Chemistry, Johannes Gutenberg University of Mainz, Duesbergweg 10–14, 55128 Mainz, Germany.
Email: sebastian.seiffert@uni-mainz.de

Funding information
Bundesministerium für Bildung und Forschung, Grant/Award Number: 02WME1613

Abstract

The polymerization of *N*-acryloyl glycineamide (NAGA) in water results in the creation of robust supramolecular hydrogels, exhibiting a network structure through inter-chain crosslinking formed by hydrogen bonds between NAGA units. The stability of these hydrogen bonds in water is based on the aggregation of NAGA units into microdomains or clusters, thereby effectively shielding the hydrogen bonds from the surrounding aqueous medium. Beyond the inherent water absorption characteristics of these hydrogels, the unique ability for the dissociation and re-association of their physical crosslinks imparts features such as reversible swelling and shrinking as well as self-healing and remolding capabilities. In this study, we synthesize a series of supramolecular hydrogels through copolymerization of NAGA and ionic sodium acrylate comonomers for a dual purpose: first, to regulate water absorption levels, and second, to introduce a salt partitioning effect into the hydrogels during their swelling in salt solution. Our findings indicate that the properties of these hydrogels are intricately influenced by the volume fraction of the solid network, the concentration of ionic units, and temperature. Notably, supramolecular samples with ionic units exhibit a 16% salt rejection in a single cycle of salt partitioning during their swelling in a 1 $g \cdot L^{-1}$ sodium chloride solution.

KEYWORDS

salt partitioning, supramolecular hydrogels, swelling and shrinkage, thermo-responsivity

1 | INTRODUCTION

Supramolecular hydrogels belong to a unique category of materials. Apart from sharing common traits with hydrogels, such as water absorption and retention, they exhibit characteristics typical of transient supramolecular materials, including responsiveness to stimuli, self-healing capabilities, and recyclability.[1,2] The transient nature of inter-chain crosslinks also imparts a potential for reversible swelling and shrinking to these materials. An additional promising application for supramolecular hydrogels lies in water purification and desalination.[3] In that type of application, their inherent self-healing and recyclability sets them apart from chemically crosslinked counterparts, offering a substantial increase in the lifetime of these materials. This particular feature is crucial for steering these processes toward greater sustainability.

While the dynamic nature of physical crosslinks imparts intriguing features to supramolecular hydrogels, it comes at the expense of stability. In particular,

hydrogen bonds pose a significant challenge, as they tend to easily dissociate in aqueous environments. To enhance stability, a key approach involves increasing the number of hydrogen bonds forming each crosslinking junction and protecting them from surrounding water through aggregation.[4] This stabilization strategy finds ample evidence in nature. In our body, where water constitutes approximately 60%, the structural integrity and essential functions of biological systems like DNA and proteins rely on numerous intra and inter-chain hydrogen bonds. These interactions are further reinforced by base-stacking interactions between aromatic nucleobases and the hydrophobic effects.[5] Taking inspiration from these instances, various synthetic functional groups have been incorporated for the creation of hydrogen-bonded supramolecular hydrogels. Among these, for example, the ureidopyrimidinone (UPy) group stands out as one of the most recognized. When one UPy group assembles with another, it forms four hydrogen bonds with a dissociation constant and equilibrium constant in the order of $\sim 10^{-1}\ s^{-1}$ and $10^{8}\ M^{-1}$, respectively, in a nonpolar medium or in bulk.[6] However, the presence of water weakens the UPy-UPy interactions, rendering UPy-based hydrogels unstable in aqueous environments. To counteract this effect, UPy groups need protection, achieved, for instance, by introducing a hydrophobic spacer to the polymer backbone. The resulting phase separation between hydrophobic and hydrophilic components creates a protective layer that isolates UPy-based self-assembled segments from the surrounding water.[7]

N-acryloyl glycinamide (NAGA) is a functional group with the capacity to create robust hydrogels through the establishment of inter-chain hydrogen bonds during polymerization in an aqueous environment. Haas and Schuler were the pioneers in introducing both the monomer and its corresponding polymers and hydrogels.[8,9] The stability of hydrogen bonds in NAGA hydrogels can be attributed to two crucial factors. First, a single NAGA unit can establish four hydrogen bonds with two other NAGA units. Second, the further aggregation of these hydrogen bond motifs leads to distinct microdomains or clusters, effectively shielding the hydrogen bonds from water molecules.[10] NAGA-based hydrogels commonly display an upper critical volume phase transition temperature, typically occurring in the range of 20–35°C, due to the partial dissociation of hydrogen bonds at elevated temperatures and their capacity for re-association at lower temperatures.[11–14] The stability of NAGA hydrogels, even without chemical crosslinkers, and their thermoresponsive nature position this functional group as a promising choice for creating hydrogen-bonded supramolecular hydrogels in various applications, such as bio applications or the design of hydrogels with self-healing abilities.[15,16]

Through the incorporation of NAGA with other monomeric units such as acrylic acid, acrylamide, *N*-isopropyl acrylamide, glycidyl methacrylate, and acrylamide-2-methylpropanesulfonic, either in the form of random or block copolymers interpenetrating networks, or micro- and nanogels one can tailor the thermoresponsivity and other characteristics of the resulting hydrogels, including mechanical properties.[13,14,17–24] The copolymerization of NAGA with monomers such as acrylic acid or methacrylic acid results in hydrogels that exhibit not only temperature responsiveness but also pH sensitivity. Moreover, the presence of (meth)acrylic acid, particularly in its ionic state, enhances the osmotic pressure of the hydrogels. This characteristic makes these hydrogels well-suited for applications such as forward osmosis-based water desalination.[3,25] The transition temperature of NAGA polymers is notably influenced by the presence of (meth)acrylic acid. This influence is highly dependent on both the protonation state and the concentration of comonomers. In general, when comonomers are in the ionic state and their concentration is below 30 mol%, an increase in the comonomer content results in a reduction of the transition temperature.[13,14] In addition, the presence of these ionic components may lead to competitive interactions, subsequently compromising the stability of NAGA inter-chain crosslinks. To (partially or fully) offset this effect, it becomes essential to elevate the level of hydrogen bond aggregation and promote the formation of microdomains/clusters. Elevating the concentration of the monomer solution during the gelation process, thereby increasing the volume fraction of the solid network in the resulting hydrogels (φ_0), is a method to enhance the level of aggregation. It is established that augmenting φ_0 leads to a higher degree of chain entanglements within the hydrogel network.[26,27] These entanglements play a role in raising phase separation between hydrogen bonds and either ionic comonomers or the surrounding water, consequently boosting the stability of the hydrogels.

This investigation explores the impact of sodium acrylate (SA) as an ionic comonomer on the stability of NAGA-based hydrogels. A diverse array of supramolecular hydrogels is synthesized for this purpose, systematically varying both the content of sodium acrylate (C_{SA}) and φ_0. The examination of the impact of φ_0 on the stability of NAGA hydrogels was infrequently explored. Furthermore, unlike the majority of studies, this research initially neutralizes the acrylic acid comonomers with sodium hydroxide during the polymerization solution. Subsequently, in subsequent experiments, the pH of water is maintained at around seven to prevent the protonation of sodium acrylate comonomers. The properties of these hydrogels, encompassing stability, water absorption, swelling and shrinkage, plateau modulus, as well as

remolding and self-healing abilities, are measured and discussed. The findings demonstrate that all features of the hydrogels can be finely controlled and adjusted by manipulating C_{SA}, φ_0, and the temperature of the experiments. Additionally, hydrogels incorporating ionic units exhibit salt partitioning during swelling in a salt solution, showcasing their potential for brackish water desalination.

2 | EXPERIMENT

2.1 | Materials

Glycinamide hydrochloride (97%), acrylic acid (97%), potassium carbonate, magnesium sulfate, acryloyl chloride (97%), dried methanol, acetone, ammonium persulfate, and tetramethylethylenediamine are purchased from Aldrich or Fischer scientific and used without further purification.

2.2 | Synthesis of *N*-acryloyl glycinamide

NAGA is synthesized following the method outlined by Guo et al.[11] In summary, in a 500 mL three-necked flask, 12.58 g (114 mmol) of glycinamide hydrochloride, 12.76 g (227 mmol) of potassium hydroxide, 4.69 g (34 mmol) of potassium carbonate, and 28.63 g (238 mmol) of magnesium sulfate are dispersed in 130 mL of dry methanol. Placing the flask in an ice bath, 11.26 g (124.5 mmol) of acryloyl chloride, dissolved in 155 mL of diethyl ether, is added dropwise to the dispersion over 4.5 hours under vigorous stirring. The ice bath is then removed, and the dispersion is further stirred overnight. After removing diethyl ether with a rotary evaporator, 125 mL of methanol is added to the flask, and the dispersion is heated to 50°C. The hot dispersion is filtered to obtain a colorless solution. Subsequently, the methanol is evaporated using the rotary evaporator, and the resulting solid is dried under vacuum. This solid is then mixed with hot acetone for 15 minutes and filtered to extract the product. The acetone is evaporated to obtain the product, and the filtered-off solid is once again mixed with fresh hot acetone. This procedure is repeated at least three times. Finally, to eliminate the residue of impurities from the product, it undergoes recrystallization from isopropanol. ^{1}H NMR (400 MHz, DMSO-d6): 3.72 (d, NH—C$\underline{H}_2$—C═O), 5.57 (dd, C$\underline{H}$H—CH—C═O), 6.09 (dd, CH$\underline{H}$—CH—C═O), 6.29 (dd, CH_2—C$\underline{H}$—C═O), 7.01 (s, CH_2—C═O—N$\underline{H}$H), 7.37 (s, CH_2—C═O—NH$\underline{H}$), 8.25 (s, N$\underline{H}$—CH2—C═O).

2.3 | Synthesis of supramolecular hydrogels

Hydrogels are fabricated through free radical polymerization utilizing a redox system at room temperature. The quantity of *N*-acryloyl glycinamide is held constant at 1 g (7.80 mmol). The amounts of sodium acrylate and water are adjusted to achieve the desired mole fraction of ionic units and monomer concentration, respectively. The quantity of ammonium persulfate (APS) is adjusted to maintain a molar ratio with monomers of 0.008. Following the dissolution of NAGA, sodium acrylate, and ammonium persulfate in water, the solution is purged with nitrogen for 30 minutes. Subsequently, a predetermined amount of tetramethylethylenediamine (10 times that of ammonium persulfate) is introduced to initiate gelation at room temperature. Gelation becomes apparent in all reactions within a few minutes of tramethylethylenediamine (TEMED) addition. The reactions are left to proceed overnight. Subsequently, the hydrogels are immersed in deionized water to dissolve any unreacted monomers and linear chains. Finally, the hydrogels are dried at 60°C under reduced pressure.

2.4 | Swelling and shrinking experiments

For assessing the hydrogel swelling capacity, 100 mg of dried sample is placed within a polyamide sheet with a 50 μm pore size. The sheet is folded, securing an octagon-like shape with clamps to prevent sample material from escaping. Subsequently, the samples are immersed in water or a salt solution at a controlled temperature. The mass of swollen hydrogels is recorded every 30 minutes during the initial 6 hours of the experiment. Afterwards, the samples are left in the water for an additional 18 hours, with their mass measured once again during this period. Hydrogel swelling is determined by the formula:

$$Q = \frac{m_h - m_d}{m_d}, \quad (1)$$

where m_h and m_d represent the mass of swollen hydrogels and dried hydrogels, respectively. The ultimate Q value is regarded as the equilibrium swelling.

To evaluate the degree of hydrogel shrinkage, the hydrogels are initially heated to either 20°C or 50°C and left at the corresponding temperature for 12 hours to achieve equilibrium swelling. After measuring water absorption, the hydrogels are then cooled down to 5°C

and left for another 12 hours. Subsequently, the hydrogels are weighed to calculate the water content.

2.5 | Rheological assessment

The plateau modulus of the hydrogels is determined through a shear rheology experiment using a stress-controlled Anton Paar MCR 302 rheometer. In each measurement, the sample undergoes a 30-minute time-sweep experiment ($\gamma = 0.1\%$, $\omega = 1$ rad·s^{-1}). Following this, an amplitude sweep is conducted at a constant frequency of $\omega = 1$ rad· s^{-1} to establish the linear viscoelastic regime ($\gamma = 0.001$–1%). To ensure that the preceding amplitude sweep hasn't induced time-dependent changes in the sample, another 10-minute time-sweep experiment is performed ($\gamma = 0.1\%$, $\omega = 1$ rad· s^{-1}). Subsequently, a frequency-sweep experiment is carried out with a constant strain amplitude ($\gamma = 0.1\%$, $\omega = 0.1$–100 rad· s^{-1}).

The evaluation of the hydrogel self-healing ability also involves shear rheology. This experiment comprises multiple time-sweep tests in the non-linear viscoelastic regime, each followed by a time-sweep experiment in the linear viscoelastic regimes ($\gamma = 0.1\%$, $\omega = 1$ rad· s^{-1}). The procedure begins with a 10-minute time-sweep measurement at the linear viscoelastic regime. The second test is conducted by adjusting the strain amplitude to 10% for 10 minutes, placing all samples in the non-linear viscoelastic regime at this amplitude. Following the third test in the linear viscoelastic regime ($\gamma = 0.1\%$), the shear deformation increases to 50%. This protocol is repeated for shear amplitudes of 100%, 200%, 400%, and 600%, each lasting 10 minutes, as the third, fourth, fifth, and sixth time-sweep measurements in the non-linear regime. The final step of this experiment is a time-sweep measurement at $\gamma = 0.1\%$.

2.6 | Remolding of samples

For the remolding of hydrogels, the top part of a 6 mL syringe is removed, and dried samples are placed into the syringe. Subsequently, an appropriate amount of water is added to achieve a volume fraction of dried samples set to 0.1. To ensure the complete sealing of dried hydrogels and water, the plunger of another syringe is inserted into the syringe from the upper, cut side. After the hydrogels absorb water, the position of the swollen samples is adjusted within the syringe. The syringe is then immersed in a water bath at a temperature of 90°C for 30 minutes, applying gentle pressure on the upper plunger and, consequently, on the swollen hydrogels. Finally, the upper plunger is removed, allowing the remolded samples to be easily pushed out of the syringe.

2.7 | Salt fractionation experiment

The salt fractionation of hydrogels is measured as described previously.[25] In summary, dry hydrogels are put in a NaCl salt solution with a concentration of $C_S = 0.017$ mol·L^{-1} (1 g·L^{-1}) as a model brackish water with a volume of $2 \times Q_{eq} \times m_d$, where Q_{eq} and m_d are the equilibrium degree of swelling and the mass of the dry hydrogels, respectively. Therefore, at the swelling equilibrium, the volume of the supernatant phase equals the volume of the absorbed solution by the hydrogels. Then, the hydrogels are removed from the solution and concentration of the supernatant phase is estimated by measuring their ionic conductivity (FiveEasy Plus Conductivity meter FP30-Std-Kit; Mettler Toledo) and comparison of the obtained data with a calibration curve constructed by the ionic conductivity of reference NaCl solutions with a concentration of 0.2–20 g·L^{-1}.

3 | RESULTS AND DISCUSSION

3.1 | Hydrogel synthesis and effective crosslinking density

The NAGA monomer is synthesized with a high purification, confirmed by ^{1}H NMR, which is demonstrated in Figure S1 in the supporting information. Hydrogels are prepared through the random copolymerization gelation of NAGA and SA at room temperature as illustrated in Scheme 1. Two parameters are deliberately altered across the samples: (i) the mole content of ionic comonomers (C_{SA}), set at 0, 2, 5, and 10 mol%, and (ii) the volume fraction of the network in gelation (φ_0), set at 0.1, 0.15, and 0.2. Subsequently, the samples are formulated as NGSAC_{SA}_φ_0. In all reactions, a solid-like gel is achieved, exhibiting no flow in the vial inversion test. The absence of a chemical crosslinker in the preparation of these samples highlights that the formation of the gel during the polymerization of NAGA and SA monomers underscores the stability of NAGA hydrogen-bonded inter-chain crosslinks in all samples as depicted in Scheme 1. Generally, individual, non-protected hydrogen bonds experience a significant weakening in water due to their low energy of dissociation. For instance, the dissociation energy of a single amide hydrogen bond in water for a model β-sheet is 0.23 kJ·mol^{-1}. The stability of NAGA hydrogen bonds in water, as described by Dai et al., originates from the aggregation of hydrogen bonds into clusters, effectively shielding them from direct contact with water molecules.[10] In hydrogen-bonded supramolecular hydrogels, such as the samples examined in this study, not only does the gel formation rely on the mentioned aggregates, but all other physical and mechanical

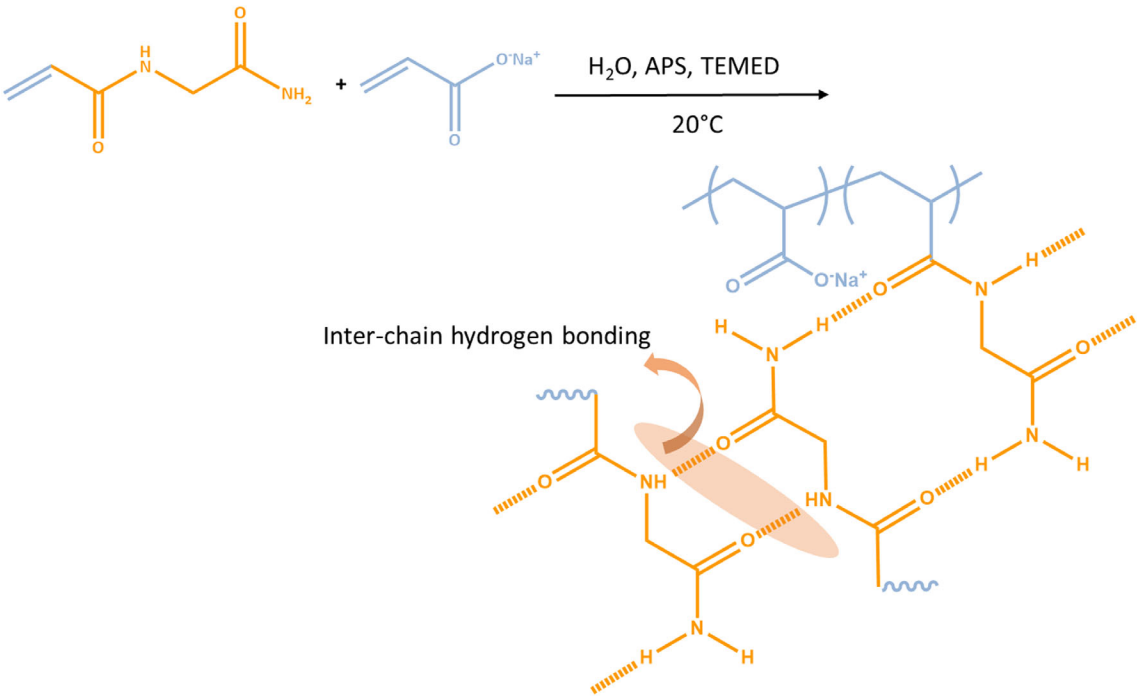

SCHEME 1 Polymerization of NAGA and sodium acrylate in water. Each NAGA unit establishes four hydrogen bonds with two additional NAGA units. These inter-chain hydrogen bonds serve as physical crosslinks, resulting in the formation of a network structure.

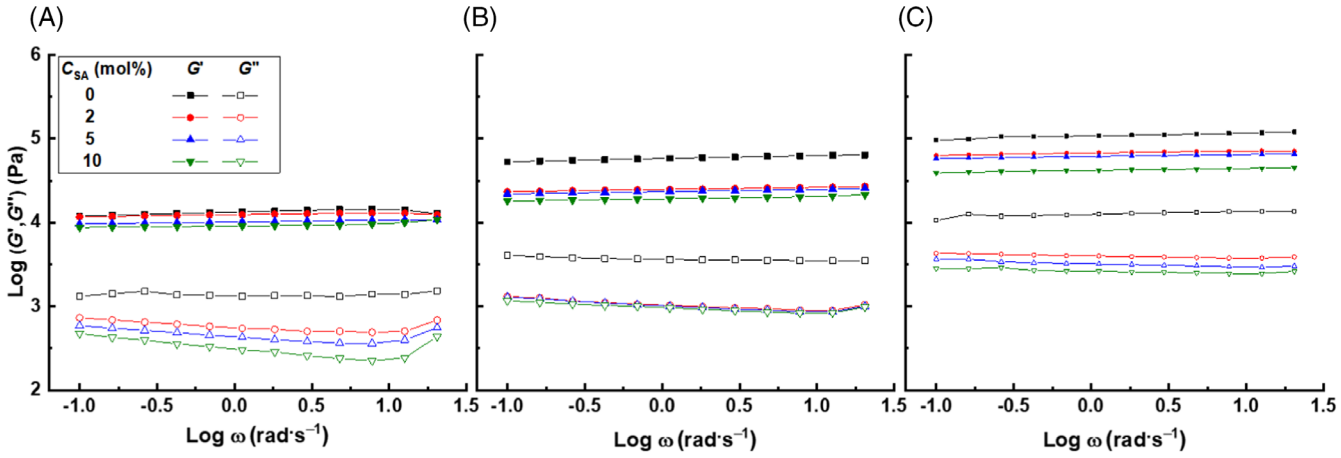

FIGURE 1 Dynamic moduli of the investigated hydrogels derived from a frequency-sweep shear rheology experiment conducted at 20°C. The volume fraction of the network in hydrogels (φ_0) are (A) 0.1, (B) 0.15, and (C) 0.2.

properties depend on their stability. The potential disaggregation of these structures, coupled with the subsequent dissociation of hydrogen bonds, occurs under applied conditions such as pH variations, temperature changes, or exposure to shear force.

For a comprehensive understanding of the degree of NAGA aggregation, the mechanical properties of the synthesized hydrogels are assessed through shear rheology at 20°C. The outcomes are illustrated in Figure 1. This measurement is conducted because any aggregate that connects two polymer chains acts as an effective crosslinker, thereby influencing the plateau modulus of hydrogels according to.

$$G(\varphi) \cong \upsilon_c RT \varphi_0^{0.66} \varphi^{0.33}, \quad (2)$$

where ν_c, φ_0 and φ represent the density of crosslinking points, the volume fraction of polymers in the as-prepared gel, and the volume fraction in the measured state, respectively.[28] Given that $\varphi = \varphi_0$, the measured moduli are directly proportional to ν_c and φ_0:

TABLE 1 Plateau modulus (G), and crosslinking density (ν_c) data for investigated hydrogels with φ_0 values of 0.1, 0.15, and 0.2 and C_{SA} of 0, 2, 5, and 10 mol%.

	φ_0	C_{SA}= 0 mol%	C_{SA} = 2 mol%	C_{SA} = 5 mol%	C_{SA} = 10 mol%
G (kPa)	0.1	13.4	12.5	10.2	9.1
	0.15	58.3	24.9	23.5	19.2
	0.2	108.6	67.8	61.8	42.1
ν_c (mol·m^{-3})	0.1	54.23	50.32	41.37	36.61
	0.15	117.65	50.32	47.42	38.82
	0.2	146.08	91.16	83.15	56.63

$$G(\varphi) \cong \upsilon_c RT\varphi_0. \quad (3)$$

During the frequency sweep measurement in shear rheology, all samples exhibit a rubbery plateau within the frequency range of 0.1–100 rad·s^{-1}. The measured plateau moduli obtained from the rheology test, along with the crosslinking density determined using equation 3, are compiled in Table 1. In a broad sense, the plateau modulus of the hydrogels under investigation demonstrates an increase with the elevation of φ_0, aligning with the predictions from equation 3. This parameter plays a role in influencing the extent of chain entanglement. Moreover, at a constant φ_0, the plateau modulus experiences a decrease with the rise in SA content. Referring to equation 3, this decline is likely attributed to the reduction in crosslinking density. This reduction is linked to the presence of competitive interactions between NAGA and SA. These interactions, in turn, disrupt a portion of NAGA hydrogen bonds, leading to a decrease in the density of hydrogen bonds and the disarray of NAGA-NAGA interactions, which is crucial for the formation of stable aggregates. This effect is more pronounced in samples prepared with higher φ_0, indicating a greater extent of stability. The impact of ionic comonomers on hydrogen bond stability can be investigated through FTIR experiments. Figure 2 illustrates the results of this analysis for samples synthesized at $\varphi_0 = 0.2$. The peak associated with C═O stretching is observed at 1626 cm^{-1} for sample NGSA0_0.2. With the addition of 2 mol% ionic comonomers, this peak shifts to 1645 cm^{-1}. This upward shift in wavenumbers suggests a reduction in hydrogen bond strength.[13] This trend is further evident with an increase in comonomer content to 10 mol%. The weakened hydrogen bonding results in decreased stability, leading to a reduction in the number of hydrogen bonds contributing to the formation of NAGA aggregates. Consequently, the heightened presence of ionic comonomers contributes to a lower density of stable NAGA aggregates, causing a subsequent decrease in crosslinking density. It is noteworthy that this reduction in crosslinking density may cause the copolymer chains to partially dissolve in water over time, serving as a criterion for hydrogel instability in this study.

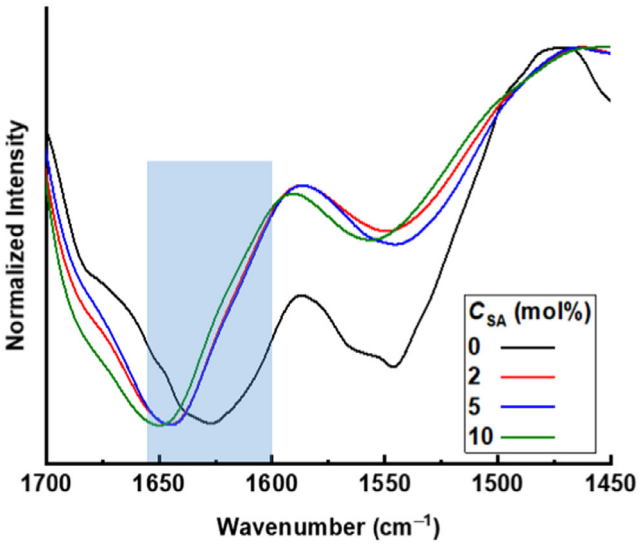

FIGURE 2 FTIR spectra of hydrogels with $\varphi_0 = 0.2$. By increasing the ionic comonomers, the C═O stretching peak in the region of 1600–1650 cm^{-1} shifts to higher wavenumbers.

3.2 | Stability in water, water absorption, and water release

A key characteristic of hydrogels lies in their capacity for water absorption and retention. When a dry hydrogel is introduced into water or a salt solution, the water absorption persists until the osmotic pressure of the swollen sample aligns with the osmotic pressure of the surrounding medium. At this equilibrium swelling state, further water absorption ceases. The examination of water absorption in water at 20°C for the studied hydrogels reveals that certain hydrogels exhibit instability in water, with some partially dissolving before attaining equilibrium, illustrated for sample NGSA10_0.1 in Figure S1 in

TABLE 2 The stability of investigated hydrogels in water in relation to the volume fraction of network, (φ_0), SA content (C_{SA}), and temperature (T). Hydrogels exhibiting stability at the respective temperatures are denoted in green.

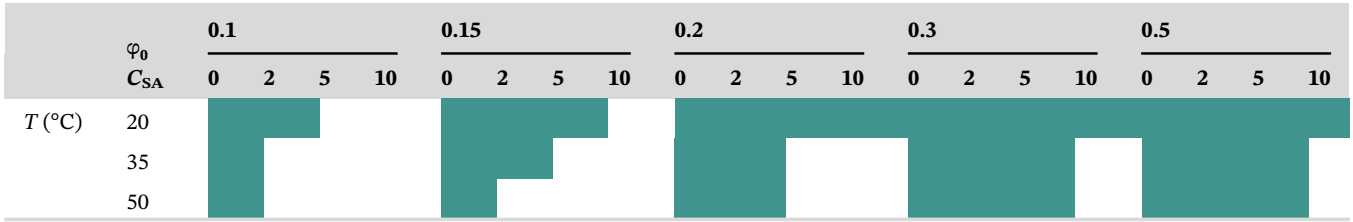

the supporting information as an example. This phenomenon stems from the potential instability of physical crosslinks during water absorption. As the water content within the hydrogel network increases, the likelihood of interactions between water and NAGA units rises. These competitive interactions have the potential to decrease the mole fraction of NAGA-NAGA hydrogen bonds and alter the arrangement of NAGA interactions necessary for NAGA aggregation. Both of these effects contribute to the instability of NAGA aggregates and a reduction in the number of network junctions, which may lead to the dissociation of NAGA hydrogen bonds. The decrease in crosslinking density during water absorption leads to a transition from a gel to a sol state if the crosslinking density falls below the minimum threshold needed for gel formation. Furthermore, temperature significantly impacts the stability of both individual NAGA hydrogen bonds and NAGA aggregates. To explore this influence, the stability of hydrogels is examined not only at room temperature but also at elevated temperatures of 35°C and 50°C. The findings are outlined in Table 2. The reference samples, devoid of ionic comonomers and synthesized across all studied φ_0 values, exhibit stability up to 50°C. This affirms the efficient aggregation of NAGA units, even at a low φ_0 of 0.1. However, in this volume fraction, the presence of a small amount of ionic groups can destabilize these aggregates, as evidenced by the instability of sample NGSA2_0.1 at 35°C and 50°C. With a further increase in C_{SA}, samples (NGSA5_0.1 and NGSA 10_0.1) prove to be unstable even at 20°C. However, this destabilizing effect of the ionic comonomer can be compensated by increasing φ_0 as confirmed by higher stability of corresponding hydrogels with comparable ionic group content. In light of the fact that hydrogels with 5 or 10 mol% SA partially dissolved in water at 35°C and 50°C, a new series of hydrogels with $\varphi_0 = 0.3$ and $\varphi_0 = 0.5$ is synthesized. Elevating φ_0 to 0.3 renders the sample with 5 mol% SA completely stable in water at 35°C and 50°C. However, the sample with 10 mol% SA still exhibits partial dissolution in water. Further increasing φ_0 to 0.5 does not contribute to the stabilization of the sample with 10 mol% SA at high temperatures. The synthesis of hydrogels with $\varphi_0 > 0.5$ is disregarded due to the high viscosity of the polymerization solution and the potential for inadequate mixing of components before the polymerization process commences. In summary, based on the overview provided in Table 2, the stability of hydrogels is controlled by φ_0, C_{SA}, and the experimental temperature. These factors collectively influence the crosslinking density of hydrogels. It is noteworthy that in hydrogels containing SA, aside from the formation of competitive NAGA-SA interactions, ionic comonomers contribute to an elevation in the osmotic pressure of hydrogels and the quantity of absorbed water. This, in turn, intensifies the competitive interactions between water and NAGA.

Based on the outcomes of the hydrogel stability tests, the equilibrium swelling of samples is assessed at 20°C and 50°C for those samples exhibiting stability at these temperatures. Additionally, this parameter is measured at 5°C for all samples. The findings are depicted in Figure 3. In the Flory-Rehner theory, at the equilibrium swelling state, three components of the osmotic pressure of hydrogels—namely enthalpic, entropic, and ionic terms—should equilibrate.[29] According to this theory, equilibrium swelling maintains a direct correlation with the content of ionic comonomer due to its impact on the ionic term of the osmotic pressure of gels. Furthermore, equilibrium swelling exhibits an inverse correlation with the crosslinking density of the network (ν_c) and φ_0, attributed to their influence on the entropic term of the osmotic pressure of gels. These relationships are evident in the equilibrium swelling data of the examined samples: at a specified φ_0, Q_{eq} rises with an increase in SA content. Similarly, with fixed C_{SA}, Q_{eq} diminishes as φ_0 increases. Beyond the common effects of φ_0 and C_{SA} on the osmotic pressure of hydrogels, shared with chemically crosslinked hydrogels, the specific impact of these parameters on the crosslinking density in supramolecular hydrogels, as discussed in the context of hydrogel stability, must be considered. This influence, leading to a change in the mole fraction of inter-chain crosslinks, has an additional effect on the values of equilibrium swelling. Along this line, temperature, as another variable, should

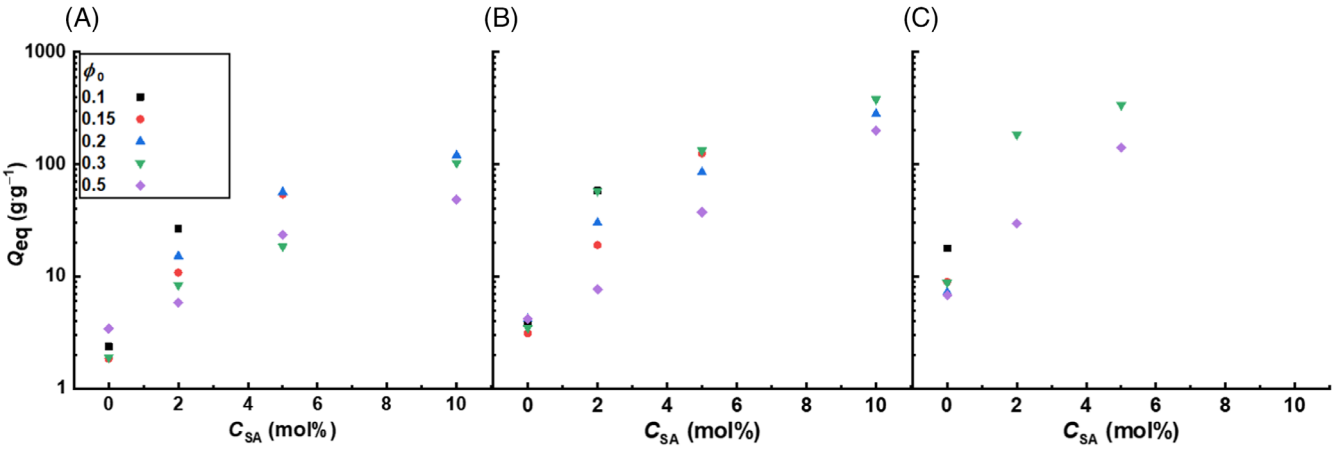

FIGURE 3 Equilibrium swelling (Q_{eq}) of investigated hydrogels in DI-water relation to the network volume fraction (φ_0) and SA content (C_{SA}) at temperatures of (A) 5°C, (B) 20°C, and (C) 50°C.

also be taken into account. As observed in the data presented in Figure 3, the elevation in temperature markedly influences the equilibrium swelling of stable hydrogels. This effect arises from the potential dissociation of hydrogen bonds at high temperatures, which results in a significant impact on the crosslinking density of hydrogels.

The hydrogen bonds that undergo dissociation upon heating have the potential to reassociate under suitable conditions, involving the provision of activation energy for bond formation and a decrease in temperature. Consequently, beyond the swelling of hydrogels upon heating, they can also undergo shrinkage upon cooling. In this context, the extent of hydrogel shrinkage emerges as a crucial parameter for all relevant applications. To explore this parameter, after determining Q_{eq} at 5°C, samples are subjected to heating up to 20°C or 50°C (T_2) to attain the equilibrium state. Subsequently, the hydrogels are cooled back down to 5°C, and Q_{eq} at this temperature is once again measured. This particular equilibrium swelling is denoted as Q_{eq} (5,C) to distinguish it from the initial measurement before heating. The extent of shrinkage is assessed by comparing the amount of released water during hydrogel shrinkage with the equilibrium swelling of hydrogels at T_2 ($T_2 = 20$°C or 50°C):

$$V_{sh} = \frac{Q_{eq}(T_2) - Q_{eq}(5,C)}{Q_{eq}(T_2)}. \quad (4)$$

The V_{sh} ratio illustrates the proportion of adsorbed water at 20°C or 50°C that can be released upon cooling the hydrogels to 5°C. To offer a more fundamental perspective, the numerator of V_{sh} can be compared with the amount of water absorption during heating from 5°C to T_2:

$$V_{reass} = \frac{Q_{eq}(T_2) - Q_{eq}(5,C)}{Q_{eq}(T_2) - Q_{eq}(5)}. \quad (5)$$

The increase in water absorption during heating stems from the dissociation of hydrogen bonds, resulting in a reduction of the crosslinking density. Consequently, V_{reass} can be regarded as a criterion that indicates the proportion of dissociated hydrogen bonds during heating from 5°C to T_2, which can be reassociated during cooling from T_2 to 5°C. In an extreme scenario, if no hydrogen bonds can reform, Q_{eq} (5,C) = Q_{eq} (T_2), leading to $V_{reass} = 0$. In the opposite scenario, if all dissociated hydrogen bonds can reform, Q_{eq} (5,C) = Q_{eq} (5) and $V_{reass} = 1$.

The data for V_{sh} and V_{reass} are depicted in Figure 4, illustrating their dependence on φ_0, C_{SA}, and the experimental temperature. In a broad trend, both V_{sh} and V_{reass} exhibit a decrease with an increase in ionic units, attributed to their impact on the instability of hydrogen bonds through the formation of competitive NAGA-SA interactions. The heightened instability of hydrogen bonds leads to a reduced likelihood of stable hydrogen bonds reforming and the recovery of the initial crosslinking density. A similar effect is observed for the parameter φ_0 as well: an increase in φ_0 generally enhances the extent of shrinkage and the proportion of hydrogen bond re-association. Despite the substantial impact of temperature on the instability of hydrogen bonds, the influence of this parameter on V_{sh} and V_{reass} does not align with the observed trend for the other two influential parameters. Upon comparing the data, it becomes evident that V_{sh} and V_{reass} exhibit significant improvement when hydrogels are heated to 50°C and subsequently cooled down to 5°C. This observation could be attributed to the activation energy necessary for the re-association of NAGA

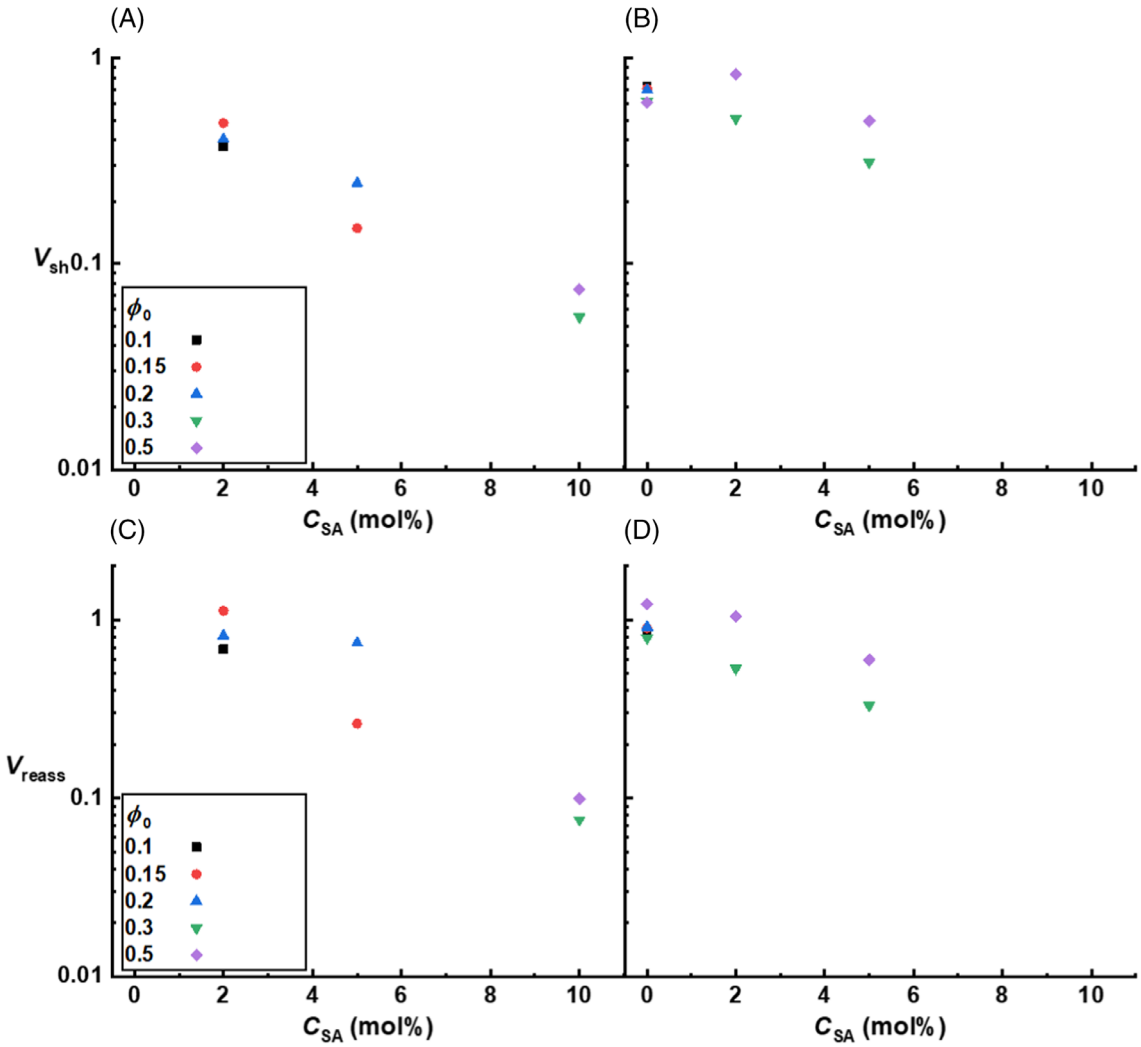

FIGURE 4 The level of hydrogel shrinkage (V_{sh}) and the ratio of the difference in equilibrium swelling in DI-water during cooling and heating (V_{reass}) for hydrogels with different φ_0 and C_{SA}. (A and C) cooling from 20°C to 5°C. (B and D) cooling from 50°C to 5°C.

hydrogen bonds. While increasing the temperature to 50°C results in more dissociation of hydrogen bonds compared to heating to 20°C, the annealing process of hydrogels at 50°C to reach equilibrium provides the activation energy required for the reformation of dissociated NAGA hydrogen bonds. Additionally, the higher dynamics of polymeric chains at elevated temperatures increase the likelihood of the arrangement of NAGA units, essential for their stable aggregation. It is worth noting that the temperature increase to 50°C is applicable only to samples that remain stable at this temperature.

In addition to DI-water, the water absorption and shrinkage levels of the samples are assessed in 1 g·L^{-1} NaCl solution. The data are depicted in Figures S3 and S4 in the supporting information. The presence of salt ions diminishes the equilibrium swelling of hydrogels, providing further evidence for samples with 5 or 10 mol% of ionic comonomers. The reduced water absorption capability is attributed to the decreased difference in osmotic pressure between hydrogels and the surrounding solution. In terms of the Flory-Rehner theory, this translates to a less impact of the ionic term of the osmotic pressure. Consequently, the water absorption of samples with a higher proportion of ionic units is more susceptible to variations in salt ion concentration in the surrounding solution. This decrease in water absorption also impacts the stability of hydrogels. For instance, sample NGSA10_50, which exhibited instability in DI-water at 50°C, demonstrates stability in a 1 g·L^{-1} NaCl solution at the same temperature. The extent of shrinkage and the proportion of hydrogen bond reassociation exhibit a low dependence on the presence of ionic units. This observation may be linked to the notion that these characteristics primarily rely on the provision of activation energy for hydrogen bond reassociation rather than the water content within the hydrogels.

3.3 | Remolding of samples and self-healing under mechanical force

During the hydrogel stability test, it was observed that when the hydrogels are submerged in water, they may undergo a gel–sol transition at elevated temperatures. Additionally, the studied hydrogels exhibit a reversible alteration in water content with temperature variations, attributed to the dissociation and re-association of physical crosslinks. These observations imply that with sufficient heating, hydrogels could transition into viscous solutions (undergoing a gel–sol transition), and upon cooling such viscous solutions, the hydrogels can reform. This remolding process holds significant importance in the context of hydrogel recycling. To investigate this property, hydrogels with a $\varphi_0 = 0.1$ undergo a remolding procedure outlined in Figure S5 in the supplementary information. Firstly, samples are subjected to heating at 90°C under gentle pressure. Subsequently, the samples are cooled to room temperature, and their mechanical properties are assessed through shear rheology. Before conducting the rheology experiment, the weight of all samples is monitored to ensure that no water evaporation occurs during the remolding process. In this analysis, all samples demonstrate a plateau modulus across the studied shear rate range, affirming hydrogel formation attributed to the re-association of NAGA hydrogen bonds. Furthermore, the remolded samples exhibit an amplified plateau modulus compared to their respective counterparts. This improvement may be linked to the provision of energy and time for the rearrangement of NAGA hydrogen bonds, facilitating the formation of additional crosslinking points. In an alternative remolding test, a specified quantity of water is introduced to samples with $\varphi_0 = 0.2$, altering the network volume fraction to 0.1. Subsequently, these samples undergo remolding following the described procedure. A comparison of the mechanical properties between these two sets of remolded samples indicates that the plateau modulus values for samples with identical ionic comonomer content closely align. (Figure 5).

Apart from the potential for remolding, the temporary nature of inter-chain crosslinks in NAGA samples imparts a self-healing capability to supramolecular hydrogels. The efficiency of self-healing can be characterized as the proportion of dissociated bonds that successfully reassociate during the healing process. Factors influencing the likelihood of bond reformation include parameters related to transient bonds, such as the activation energy for bond formation, dissociation and association times of transient bonds, and the dynamics of polymer chains/network segments linked to the supramolecular motifs.[30] To assess the self-healing capability of the investigated samples, a shear deformation experiment is conducted at room temperature, as detailed in the Experimental section. Figure 6A illustrates the outcomes of this test for sample NGSA10_0.15, serving as a representative example. As the density of transient crosslinking is inherently linked to the plateau modulus, the self-healing efficiency of each sample in these rheology tests (SH_{rh}) is calculated as the ratio of the plateau modulus in the last time-sweep experiment to that in the initial experiment:

$$SH_{rh} = G'_{13}/G'_{1}.$$

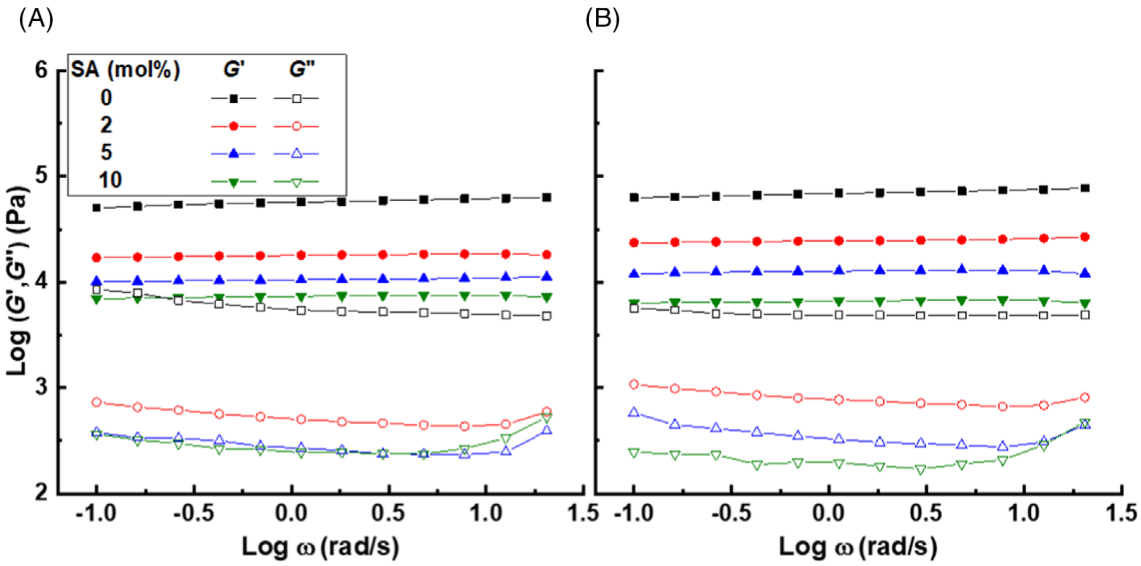

FIGURE 5 Dynamic moduli of remold samples. (A) Remolding samples with $\varphi_0 = 0.1$ to hydrogels with an identical network volume fraction. (B) Remolding of samples with $\varphi_0 = 0.2$ to hydrogels with $\varphi = 0.1$.

The representation of this data can be found in Figure 6B. As a prevailing pattern, the self-healing efficiency diminishes with the escalation of SA content, given that the ionic comonomer compromises the stability of inter-chain hydrogen bonding and the likelihood of bond reformation. Moreover, at a constant SA content, the self-healing efficiency exhibits an initial increase with the elevation of φ_0 from 0.1 to 0.15. However, it subsequently decreases upon further augmentation of φ_0 to 0.2, excluding samples NGSA0_0.15 and NGSA0_0.2. It is important to note that, on one hand, an increase in φ_0 can enhance the stability of hydrogen bonds. However, on the other hand, it can diminish the dynamics of network segments, consequently reducing the likelihood of bringing two NAGA groups into close proximity to form an inter-chain crosslink. Consequently, it could be inferred that the rise in self-healing efficiency from 0.1 to 0.15 in φ_0 is predominantly influenced by the concentration's impact on the stability of hydrogen bonds. Conversely, further increasing φ_0 to 0.2 shifts the balance toward the concentration's effect on the dynamics of network segments, resulting in a decrease in self-healing efficiency. It is worth noting that the contrasting impacts of φ_0 on self-healing efficiency can also be applied to SA content. Specifically, the destabilization of hydrogen bonding by the ionic comonomer, to some extent, contributes to the increase of network segment dynamics. The differing effects mentioned could explain why the self-healing efficiency of samples NGSAX_0.15 shows less sensitivity to changes in the content of charge groups. The intricate interplay of hydrogen bond reformation with SA content or φ_0 may account for the deviation of certain data points from the general trend observed in Figure 6B, such as the increased self-healing efficiency between samples NGSA2_0.15 and NGSA0_0.15. Contrary to the overall pattern depicted in Figure 6B, the self-healing efficiency of remold samples rises with an increase in SA content as demonstrated in Figure S6 in the supporting information. This tendency might be attributed to the prevalence of the impact of ionic units on the dynamics of polymer chains, surpassing the influence on hydrogen bond stability in remold samples.

3.4 | Salt ions fractionation

Hydrogels comprising NAGA and ionic comonomers exhibit potential salt ion partitioning during swelling in salt solution. To explore this capability, selected samples are immersed in sodium chloride solution with a concentration of 1 $g{\cdot}L^{-1}$. The experimental protocol details are explained elsewhere.[3,25] After the hydrogels reach their equilibrium state, they are separated from the remaining solution, and the conductivity of the solution is measured. This conductivity correlates with the concentration of salt ions in the supernatant phase. Furthermore, the salt rejection (SR_{sup}) can be determined by comparing the salt concentration in the supernatant phase with that in the initial salt solution.

$$SR_{sup} = \frac{C_{sup} - C_s}{C_s},$$

where C_{sup}, and C_s represent the salt concentration in the supernatant phase and the initial salt solution respectively.

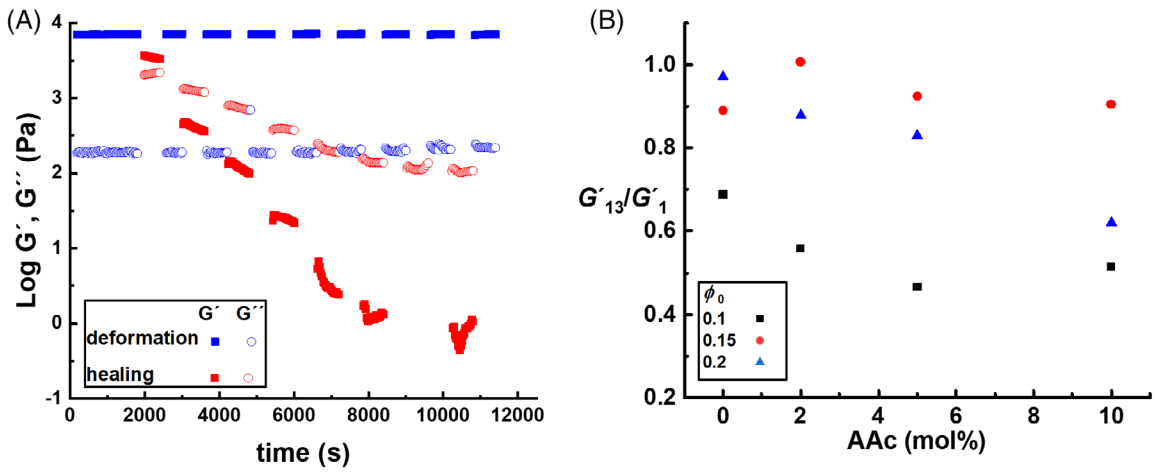

FIGURE 6 (A) Data of self-healing experiment conducted on sample NGSA10_0.15. The numbers indicate the amplitude during the deformation steps. In the other steps, the amplitude is 0.1%. (B) Efficiency of Self-healing for samples with different network volume fractions and SA content.

The concentration and salt rejection values can be compared with the prediction of Donnan theory:

$$C_{sup} = \frac{4C_s^2 + 2\rho \times C_s}{\rho + 4C_s},$$

$$SR_{sup} = \frac{\rho}{\rho + 4C_s},$$

where ρ represents the density of the ionic groups. The results, presented in Figure S7 in the supporting information, indicate that as the volume density of charge units increases, the salt rejection ability also increases. Additionally, the salt rejection data aligns well with the predictions of the Donnan equilibrium theory for the salt partitioning of charged hydrogels.

The maximum salt rejection achieved by the studied hydrogels is approximately ~16% in one cycle of salt partitioning. This means the salt concentration could be reduced to 70% and 58% of the initial salt concentration after the second and third cycles. Consequently, salt rejection could potentially reach around 42% if three salt partitioning cycles are applied. This degree of salt rejection lowers the salt content to a level within the acceptable range for drinking water.

4 | CONCLUSION

Supramolecular hydrogels feature useful characteristics such as reversible swelling and shrinking, as well as remarkable abilities for self-healing and recycling. These attributes of supramolecular hydrogels rely on non-covalent crosslinks such as hydrogen bonds and are entirely governed by the dissociation of these bonds under specific conditions, and the subsequent potential for these bonds to re-associate. Within the hydrogels studied in this work, formed through the copolymerization of NAGA and sodium acrylate, the degree and stability of these physical crosslinks are regulated by the volume fraction of the network in the prepared samples (φ_0), the content of ionic comonomers (C_{SA}), and the experimental temperature. Increasing the number of ionic units or reducing φ_0, both of which contribute to the instability of hydrogen bonds, lead to a decrease in the degree of hydrogel shrinkage and self-healing efficiency. The extent of hydrogel shrinkage is notably higher for samples that undergo annealing at 50°C and subsequent cooling to 5°C, facilitated by the provision of activation energy necessary for the reformation of hydrogen bonds. Substituting water with a 1 g·L^{-1} salt solution and thereby reducing the water content at the swelling equilibrium state enhance the stability of hydrogels. NAGA hydrogels containing ionic comonomers exhibit salt partitioning during swelling in a saline solution. Among the examined samples, a maximum salt rejection of 16% is achieved. This implies that by conducting three cycles of the salt rejection experiment, a 42% salt rejection can be attained. The Donnan theory suggests that achieving this level of salt rejection is possible in a single experimental cycle by setting the charge density of hydrogels to 0.068 mol·L^{-1}. The preparation of hydrogels with such a charge density is currently under investigation.

ACKNOWLEDGMENTS

The authors thank the German Federal Ministry of Science and Education for funding within the MEWAC framework program under project HydroDeSal (Project Code 02WME1613). Open Access funding enabled and organized by Projekt DEAL.

ORCID

Amir Jangizehi https://orcid.org/0000-0003-3829-4027
Sebastian Seiffert https://orcid.org/0000-0002-5152-1207

REFERENCES

[1] R. Dong, Y. Pang, Y. Su, X. Zhu, *Biomater. Sci.* **2015**, *3*, 937.
[2] X. Du, J. Zhou, J. Shi, B. Xu, *Chem. Rev.* **2015**, *115*, 13165.
[3] A. Jangizehi, S. Seiffert, *Macromol. Chem. Phys.* **2022**, *223*, 2200070.
[4] E. Krieg, M. M. Bastings, P. Besenius, B. Rybtchinski, *Chem. Rev.* **2016**, *116*, 2414.
[5] S. Sivakova, S. J. Rowan, *Chem. Soc. Rev.* **2005**, *34*, 9.
[6] S. H. Söntjens, R. P. Sijbesma, M. H. van Genderen, E. Meijer, *J. Am. Chem. Soc.* **2000**, *122*, 7487.
[7] P. Y. Dankers, T. M. Hermans, T. W. Baughman, Y. Kamikawa, R. E. Kieltyka, M. M. Bastings, H. M. Janssen, N. A. Sommerdijk, A. Larsen, M. J. Van Luyn, *Adv. Mater.* **2012**, *24*, 2703.
[8] H. C. Haas, N. W. Schuler, *J. Polym. Sci., Part B: Polym. Lett.* **1964**, *2*, 1095.
[9] H. C. Haas, R. D. Moreau, N. W. Schuler, *J. Polym. Sci. Part A-2: Polym. Phys.* **1967**, *5*, 915.
[10] X. Dai, Y. Zhang, L. Gao, T. Bai, W. Wang, Y. Cui, W. Liu, *Adv. Mater.* **2015**, *27*, 3566.
[11] H. Guo, C. Mussault, A. Marcellan, D. Hourdet, N. Sanson, *Macromol. Rapid Commun.* **2017**, *38*, 1700287.
[12] Z. Xu, W. Liu, *Chem. Commun.* **2018**, *54*, 10540.
[13] W. Sun, Z. An, P. Wu, *Polym. Chem.* **2018**, *9*, 3667.
[14] J. Seuring, F. M. Bayer, K. Huber, S. Agarwal, *Macromolecules* **2012**, *45*, 374.
[15] H. Wang, Y. Wu, C. Cui, J. Yang, W. Liu, *Adv. Sci.* **2018**, *5*, 1800711.
[16] H. Wang, H. Zhu, W. Fu, Y. Zhang, B. Xu, F. Gao, Z. Cao, W. Liu, *Macromol. Rapid Commun.* **2017**, *38*, 1600695.
[17] N. Majstorović, M. Zahedtalaban, S. Agarwal, *Polym. J.* **2023**, *55*, 1.

[18] N. Majstorovic, S. Agarwal, *ACS Appl. Polym. Mater.* **2021**, *3*, 4992.
[19] Q. Wu, J. Wei, B. Xu, X. Liu, H. Wang, W. Wang, Q. Wang, W. Liu, *Sci. Rep.* **2017**, *7*, 41566.
[20] D. Yang, H. Eronen, H. Tenhu, S. Hietala, *Langmuir* **2021**, *37*, 2639.
[21] S. Houben, A. A. Aldana, A.-S. Huysecom, W. Mpinganzima, R. Cardinaels, M. B. Baker, L. M. Pitet, *ACS Appl. Polym. Mater.* **2023**, *5*, 1819.
[22] S. Ge, J. Li, J. Geng, S. Liu, H. Xu, Z. Gu, *Mater. Horiz.* **2021**, *8*, 1189.
[23] T. N. Tran, S. Piogé, L. Fontaine, S. Pascual, *Eur. Polym. J.* **2022**, *173*, 111310.
[24] D. Yang, H. Tenhu, S. Hietala, *Eur. Polym. J.* **2020**, *133*, 109760.
[25] A. Jangizehi, S. Seiffert, *J. Chem. Phys.* **2021**, *154*, 144902.
[26] N. Orakdogen, O. Okay, *Eur. Polym. J.* **2006**, *42*, 955.
[27] H. Furukawa, *J. Mol. Struct.* **2000**, *554*, 11.
[28] O. Okay, *Hydrogel sensors and actuators*, Springer, Heidelberg **2009**, p. 1.
[29] P. J. Flory, *J. Chem. Phys* **1943**, *11*, 521.
[30] A. Jangizehi, M. Ahmadi, S. Seiffert, *Mater. Adv.* **2021**, *2*, 1425.

SUPPORTING INFORMATION

Additional supporting information can be found online in the Supporting Information section at the end of this article.

How to cite this article: A. Jangizehi, C. Sprenger, S. Seiffert, *J. Polym. Sci.* **2024**, *62*(19), 4443. https://doi.org/10.1002/pol.20240336